Journal of Robotics and Control (JRC)
Volume 5, Issue 6, 2024
ISSN: 2715-5072, DOI: 10.18196/jrc.v5i6.23159

Enhanced Dynamic Control of Quadcopter PMSMs Using an ILQR-PCC System for Improved Stability and Reduced Torque Ripples

Ziyaad H. Saleh [1], Basim Ghalib Mejbel [2], Ahmed Dheyaa Radhi [3], Abdulghafor Mohammed Hashim [4], Taha A. Taha [5*], Nurettin Gökşenli [6], Abadal-Salam T. Hussain [7], Ravi Sekhar [8]
[1] College of Petroleum and Minerals Engineering, Tikrit University, Iraq
[2] Al Hikma University College, Baghdad, Iraq
[3] College of Pharmacy, University of Al-Ameed, Karbala PO Box 198, Iraq
[4] Al-Amarah University College, Engineering of Technical Mechanical Power Department, Maysan, Iraq
[5] Renewable Energies Researches Unit, Northern Technical University, Kirkuk, Iraq
[6] Vocational school, Cankiri Karatekin University, 18100, Turkey
[7] Department of Medical Instrumentation Techniques Engineering, Technical Engineering College, Al-Kitab University, Altun Kupri, Kirkuk, Iraq
[8] Symbiosis Institute of Technology (SIT) Pune Campus, Symbiosis International (Deemed University) (SIU), Pune, 412115, Maharashtra, India
Email: [1] ziad_1966@yahoo.com, [2] drbasimghalib@gmail.com, [3] ahmosawi@alameed.edu.iq, [4] abd.ghafoor@alamarahuc.edu.iq, [5] t360pi@gmail.com, [6] ngoksenli@karatekin.edu.tr, [7] asth2233@gmail.com, [8] Ravi.sekhar@sitpune.edu.in
*Corresponding Author

***Abstract*—Quadcopter technology has developed fast because it's flexibility and capacity for high maneuvers. What makes PMSM suitable for Quadcopter is their high power to weight ratio, reliability and efficiency. These motors allow the operation of torque and speed control which are important for stability and maneuverability in the flight of the aircraft. Nevertheless, certain and smooth flight caused by regulation of PMSM speed and current is necessary for stable and maneuverable movement. This work presents a new control strategy connecting the ILQR control to govern the speed while the PCC profit the dynamic response and control torque ripples. A comparison is made on the performance of the ILQR-PCC system with nominal Proportional-Integral (PI) control and ILQR. From the results it is evident that the ILQR-PCC system is far superior to both the PI & ILQR controller in regards to the dynamic response, the disturbances rejection capacity as well as reducing the current signal distortions hence reducing the torque ripples. Its working was evidenced in a nonlinear LQR-controlled quadcopter to track the reference accurately and to have minimum distortion in current regulation. The presented work improves the control systems of quadcopters: it introduces a reliable method that improves stability and increases the performance of the quadcopter; therefore, this paper contributes to the existing knowledge.**

Keywords*—Quadcopter Control; PMSM; ILQR; Predictive Current Control; Torque Ripple Reduction; UAV Stability.

I. INTRODUCTION

Nowadays, quadcopters have turned into an object of interest for research and development in academia as well as industry because of their broad multifunctional uses and the increasing complexity of the technologies being employed. These are called unmanned aerial vehicles (UAVs) and are widely used in different fields today: military, social, and business ones, and have different purposes – surveillance, delivery, search and rescue operations, and more. This has encouraged many companies and researcher to come with new designs that will adequately address the operational changes that come with the growing interest in quadcopters. There is a growing need therefore for improvements in the design of quadcopters that will improve on the reliability and safety of their flight [1]-[5].

Quadcopters as one of the most commonly used UAVs have certain difficulties connected with their complex and nonlinear dynamic models. Such models can be distinguished by high dynamic: they are based on six output signals and four input signals, representing the speeds of the four electric motors that control the quadcopter's flight. The control of these motors is therefore very important in ensuring the right flight path and stability is achieved making the job of the flight control engineers and Aircraft designers complex [6]-[9].

Another determinant which can greatly affect the operations of the quadcopters is the type of the used motors. PMSMs are well recognized as the most suitable motors for the Quadcopter applications, because they have high power density, high efficiency, no rotor windings and low electrical loss and very low torque pulsations [10]-[17]. These characteristics make the PMSMs more appropriate for the high demands of the UAV applications.

To manage PMSM drives various traditional control methods have been designed such as: For example, DTC is characterized by a high torque response rate, yet due to problems with the high frequency current harmonics of low order, it operates at high sampling frequency. In contrast, Field-Oriented Control (FOC) is preferred providing the fastest response times and a high stability in steady-state

operation in a large speed range. However, it is sometimes difficult to manage the transient conditions of vehicle motors using FOC especially within dynamic environments and or rapidly varying conditions [18]-[27].

A number of research works have examined the various sophisticated control techniques for improving the operation of PMSMs. For example, [28]-[36] has developed a two-layer control system for PMSMs used in electric vehicles: MPC is used in the outer loop to control the motor's speed while PI control is used in the inner loop to manage the current. From the simulation study, the proposed MPC-PI system is found to outperform other control approach and its compatibility for electric vehicles. In a like manner, [37]-[40] designed a high-speed control method employing SMC for the inner speed control and a crude hysteresis current control for the outer current loop. This approach offered good enhancement of the speed response rate and reduced overshoot to the targeted speed therefore can be applied in complex drive systems.

Other improvements were done by [41]-[46] where the author recognized the shortcomings in the conventional techniques of motor control and came up with a more effective model predictive current control for PMSMs. This method effectively eliminated the heavy computations and present ripples, which as elucidated previous, help in boosting performance according to hardware experiments and simulations. Furthermore, [47]-[52] investigated the application of state feedback controller using LQR to control speed of PMSM that, in turn, exclude periodic fluctuation in speed and torque. This approach using LQR-based technique provides a better performance than a conventional PID controller.

Continuing from the work done by LQR, [53]-[58] studied the improvement of LQR controllers with aid of computational intelligence algorithms. The paper investigated three optimization algorithms; Simulated Annealing, Grey Wolf Optimization and Reinforcement Learning to improve the performance of LQR controllers in PMSM systems. The use of these algorithms was used in numerical simulations in Matlab/Simulink where it was observed that the LQR controllers designed in this way performed better than the basic LQR approach by providing a more fine-tuned and effective means of control.

These studies are therefore indicating the need to implement direct motor control strategies for the countries that want fast and accurate response while at the same time suppressing current distortions. LQR is also identified across the literature as being important in motor drive systems for realizing adequate control of speed and torque of motors. Based on these results, this research suggests a novel approach that incorporates PCC in the inner current control loop of the drive system and, LQR for speed control in the outer loop. This is expected to give the drive system higher reliability and dynamics as a result of the selected combination. To prove the efficiency of the proposed drive system a number of comparisons were made with drive systems that are based on other controllers such as LQR and PI controllers. The outcome of the proposed system is proven by the quadcopter performance test, together the scenario-based simulations, which reveal enhanced performance and practicability of the system in dynamic UAV settings.

II. MATHEMATICAL MODEL OF THE QUADCOPTER

A quadrotor as shown in Fig. 1 consists of four rotors of equal size and shape, with each pair of opposing rotors rotating in the same direction, opposite to that of the other pair [59]-[67].

The movement of a quadrotor is governed by the forces and torques generated by the four rotors. When one of the quadcopter's motors rotates, a torque (T_i) in (1) is generated around the motor axis and a lift force (τ_i) in (2) is directed toward the z-axis that is proportional to the speed and acceleration of each propeller's rotation.

$$\tau_i = b\omega_{m_i}^{\ 2} \tag{1}$$

$$T_i = d\omega_{m_i}^{\ 2} + J_r\dot{\omega_{m_i}} \tag{2}$$

Where, J_r is the Propeller inertia (kg·m²). b is the Lift coefficient (N·s²/rad²). d is the Drag coefficient (N·m·s²/rad²). ω_{m_i} is the Mechanical speed of the (i) propeller motor (rad/s).

Consequently, four forces and torques will be generated that contribute to the movement and rotation of the quadcopter around the three coordinate axes according to the following in (3)-(4).

$$\begin{bmatrix} u_1 \\ u_2 \\ u_3 \\ u_4 \end{bmatrix} = G \begin{bmatrix} \omega_{m_1}^{\ 2} \\ \omega_{m_2}^{\ 2} \\ \omega_{m_3}^{\ 2} \\ \omega_{m_4}^{\ 2} \end{bmatrix} \tag{3}$$

$$G = \begin{bmatrix} 0 & b & 0 & -b \\ b & 0 & -b & 0 \\ -d & d & -d & d \\ b & b & b & b \end{bmatrix} \tag{4}$$

Where, $u_1$is the X-axis thrust force (N). u_2 is the Y-axis thrust force (N). u_3 is the rotation torque about z-axis (N·m). u_4 is the Z-axis thrust force (N).

To describe the positioning of any object in coordinate space, it is necessary to determine the position coordinates and orientation angles of that object within a specific coordinate system in general, there are two coordinate systems [68]-[74]. The first is system: an Earth fixed coordinate system (Oi). the second is system (b): a body fixed coordinate system (Ob). In general, it is more convenient to formulate the rotational equations of motion with regard to the body-fixed frame when modelling quadcopters. Nonetheless, the earth fixed coordinate system is used to develop the linear motion equations.

To transform the angular velocity between the two systems, the following relationships are used [4] in (5).

$$\begin{bmatrix} \dot{\phi} \\ \dot{\theta} \\ \dot{\psi} \end{bmatrix} = \begin{bmatrix} 1 & S_\phi T_\theta & C_\phi T_\theta \\ 0 & C_\phi & -S_\phi \\ 0 & S_\phi/C_\theta & C_\phi/C_\theta \end{bmatrix} \begin{bmatrix} p \\ q \\ r \end{bmatrix} \tag{5}$$

Where, $[p \quad q \quad r]$ is the angular velocity in the quadcopter body Coordinate system (rad/s). $[\dot{\phi} \quad \dot{\theta} \quad \dot{\psi}]$ is the angular

velocity in the Earth Coordinate system (rad/s). ϕ is the angle of rotation about the x-axis (rad). θ is the angle of rotation about the y-axis (rad). ψ is the angle of rotation about the z-axis (rad).

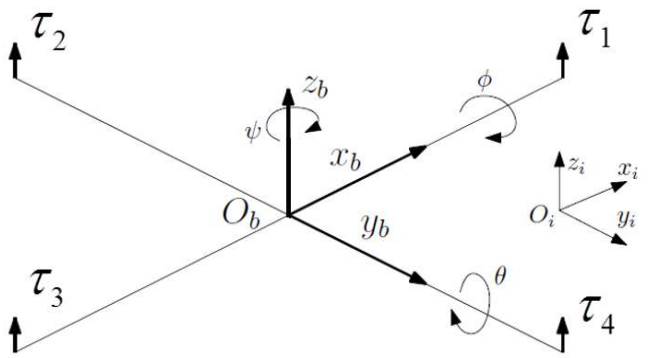

Fig. 1. Directions of rotation, and forces resulting from motors rotation

The relationship for transforming the linear velocity from the quadcopter body Coordinate system to the Earth Coordinate system is given as follows [4] in (6).

$$\begin{bmatrix}\dot{x}\\ \dot{y}\\ \dot{z}\end{bmatrix}=\begin{bmatrix}C_\psi C_\theta & C_\psi S_\theta S_\phi - S_\psi C_\phi & C_\psi S_\theta C_\phi + S_\psi S_\phi\\ S_\psi C_\theta & S_\psi S_\theta S_\phi + C_\psi C_\phi & S_\psi S_\theta C_\phi - C_\psi S_\phi\\ -S_\theta & C_\theta S_\phi & C_\theta C_\phi\end{bmatrix}\begin{bmatrix}u\\ v\\ w\end{bmatrix} \quad (6)$$

Where, $[\dot{x} \quad \dot{y} \quad \dot{z}]$ is the linear velocity in the Earth Coordinate system (m/s). $[u \quad v \quad w]$ is the linear velocity in the quadcopter body Coordinate system (m/s).

Taking into account this hybrid representation and deciding to locate the body-fixed frame's origin at the quadcopter's centre of mass, with its axes serving as the main axis of inertia, it can obtain the following nonlinear model of the quadrotor expressed in a hybrid frame [75]-[83] in (7)-(12).

$$\ddot{x} = (sin(\psi)\, sin(\varphi) + cos(\psi)\, sin(\theta)\, cos(\varphi))u_4/m \quad (7)$$

$$\ddot{y} = (-cos(\psi)\, sin(\varphi) + sin(\psi)\, sin(\theta)\, cos(\varphi))u_4/m \quad (8)$$

$$\ddot{z} = -g + (cos(\theta)\, cos(\varphi))u_4/m \quad (9)$$

$$\dot{p} = (1/I_x)(J_r q\varpi_r + lu_1 + (I_y - I_z)qr) \quad (10)$$

$$\dot{q} = \left(\frac{1}{I_y}\right)(-J_r p\varpi_r + lu_2 + (I_z - I_x)pr) \quad (11)$$

$$\dot{r} = (1/I_z)(u_3 + (I_x - I_y)pq) \quad (12)$$

Where:

$$\omega_r = -\omega_{m_1} + \omega_{m_2} - \omega_{m_3} + \omega_{m_4}$$

J_r is the propeller inertia (kg·m²). I_i is the inertia moment of the quadcopter about the i-axis (kg·m²). L is the length of the quadcopter arm (m). M is the mass of the quadcopter (kg). G is the Earth's gravitational acceleration (m/s²).

III. MATHEMATICAL MODEL OF PMSM

The mathematical model of the three-phase PMSM in a rotating two-dimensional coordinate system ω is given as follows [84]-[87] in (13)-(15).

$$i_{sd} = -\frac{R_s}{L_{sd}} i_{sd} + \omega i_{sq} + \frac{V_{sd}}{L_{sd}} \quad (13)$$

$$i_{sq} = -\frac{R_s}{L_{sq}} i_{sq} - \omega i_{sd} - \frac{\varphi_m}{L_{sq}}\omega + \frac{V_{sq}}{L_{sq}} \quad (14)$$

$$\dot{\omega} = \frac{p}{J}(T_{em} - T_L) - \frac{f}{J}\omega \quad (15)$$

Where R_s represents the stator winding resistance of the motor. $L_{sd}, L_{sq}(H)$ is the stator winding inductances along the d and q axes, respectively. $i_{sd}, i_{sq}(A)$ is the stator currents along the d and q axes, respectively. $V_{sd}, V_{sq}(v)$ is the stator voltages applied along the d and q axes, respectively. φ_m is the flux generated by the magnets in the rotor. $T_L(N.m)$ is the load torque. $f(N.m.sec/rad)$ is the coefficient of friction. $J_m(kg.m^2)$ is the moment of inertia. $T_e(N.m)$ is the electromagnetic torque.

A. Control of Quadcopter using ILQR

The control law of the linear quadratic regulator (LQR) is based on minimizing the cost function shown in the following relationship [11][14] in (16).

$$\mathrm{J} = \int_{t_0}^{t_f} [\mathrm{X(t)^T Q(t) X(t) + u^T(t) R(t) u(t)}]\, \mathrm{dt} \quad (16)$$

where Q, R are semi-defined positive diagonal weight matrices. To achieve this, the control law is defined as shown in the following relations in (17).

$$u = -K\, X \quad (17)$$

X is are the variable states, and u is the control signals (model input signals) in (18).

$$K = R^{-1} B^T P \quad (18)$$

where P is a solution of the Riccati algebraic equation in (19).

$$Q + A^T P + PA - PB R^{-1} B^T P = 0 \quad (19)$$

A and B are the dynamic and system input matrices, respectively.

To achieve high dynamic performance and accurate reference signal tracking, an integral term may be added to LQR, so it can be called ILQR. for a quadcopter, the linear model is given as in (20).

$$\dot{X}_q = A_q X_q + B_q u_q$$

where:

$$X_q = x, y, z, \emptyset, \theta, \psi, \dot{x}, \dot{y}, \dot{z}, p, q, r \text{ and } u_q = u_1, u_2, u_3, u_4.$$

$$\mathrm{A_q} = \begin{bmatrix} 0_{3\times3} & 0_{3\times1} & 0_{3\times1} & 0 & I_{3\times3} & 0_{3\times3} \\ 0_{3\times3} & 0_{3\times1} & 0_{3\times4} & 0 & 0_{3\times3} & I_{3\times3} \\ 0_{1\times3} & 0 & g & 0 & 0_{3\times3} & 0_{1\times3} \\ 0_{1\times3} & -g & 0 & 0 & 0_{3\times3} & 0_{1\times3} \\ 0_{4\times3} & 0_{4\times1} & 0_{4\times1} & 0 & 0_{3\times3} & 0_{4\times3} \end{bmatrix}, \quad (20)$$

$$\mathrm{B_q} = \begin{bmatrix} 0_{8\times1} & 0_{8\times1} & 0_{8\times1} & 0_{8\times1} \\ 1/m & 0 & 0 & 0 \\ 0 & 1/J_x & 0 & 0 \\ 0 & 0 & 1/J_y & 0 \\ 0 & 0 & 0 & 1/J_z \end{bmatrix}$$

The state space will be augmenting by adding new state variables as follows in (21)-(23).

$$\dot{\zeta}_x = x_{ref} - x \tag{21}$$

$$\dot{\zeta}_y = y_{ref} - y \tag{22}$$

$$\dot{\zeta}_z = z_{ref} - z \tag{23}$$

The state space of the quadcopter becomes as follows in (24).

$$\begin{bmatrix} \dot{X}_q(t) \\ \dot{\zeta}_q(t) \end{bmatrix} = \begin{bmatrix} A_q & 0_{12\times3} \\ -I_{3\times3} & 0_{3\times12} \end{bmatrix} \begin{bmatrix} x(t) \\ \zeta_q(t) \end{bmatrix} + \begin{bmatrix} B_q \\ 0_{3\times4} \end{bmatrix} u_q(t) + \begin{bmatrix} 0_{12\times1} \\ ref_q(t) \end{bmatrix}$$
$$ref_q(t) = \begin{bmatrix} x_{ref} \\ y_{ref} \\ z_{ref} \end{bmatrix} \tag{24}$$

The control law of quadcopter is given by the following relationship in (25).

$$u_{q^*} = -[K_{q\,4\times12} \quad K_{qI\,4\times3}] \begin{bmatrix} X_q(t) \\ \zeta_q(t) \end{bmatrix} \tag{25}$$

Fig. 2 shows the block diagram of the complete control system for a quadcopter, which consists of two stages. In the first stage, the quadcopter control signals are calculated. In the second stage, the reference speeds of the four motors are calculated to make the quadcopter move according to the desired path.

B. FOC PMSM using PI Controller

Fig. 3 shows the block diagram for controlling motor speed and currents using PI controllers. Proportional gain is utilized to enhance the rise time, while integral gain is employed to reject steady-state error. To determine these parameters, it can use several methods, including the Ziegler-Nichols method, and the internal model control approach, trial and error approach which is used in this paper [16]. In the outer regulation loop, the speed is regulated, and the reference value for the i_{sq} current is obtained, while the reference value for the i_{sd} current is zero to obtain the maximum torque of the motor [17][18]. This is followed by a sine pulse width modulation (SPWM) stage to obtain the pulses that are applied to the inverter feed the motor.

C. FOC PMSM using ILQR

To design a ILQR for speed and currents control of PMSM, the state space is given as follows in (26).

$$\begin{bmatrix} i_{sd} \\ i_{sq} \\ \omega_m \\ \zeta_{\omega_m} \\ \zeta_{isd} \end{bmatrix} = \begin{bmatrix} \frac{-R_s}{L_{sd}} & 0 & 0 & 0 & 0 \\ 0 & \frac{-R_s}{L_{sq}} & -\frac{\varphi_m}{L_{sq}} & 0 & 0 \\ 0 & \frac{1.5p^2\varphi_m}{J} & \frac{-f}{J} & 0 & 0 \\ 0 & 0 & -1 & 0 & 0 \\ -1 & 0 & 0 & 0 & 0 \end{bmatrix} \begin{bmatrix} i_{sd} \\ i_{sq} \\ \omega_m \\ \zeta_{\omega_m} \\ \zeta_{isd} \end{bmatrix} + \begin{bmatrix} \frac{1}{L_{sd}} & 0 \\ 0 & \frac{1}{L_{sq}} \\ 0 & 0 \\ 0 & 0 \\ 0 & 0 \end{bmatrix} \begin{bmatrix} V_{sd} \\ V_{sq} \end{bmatrix} + \begin{bmatrix} 0 & 0 \\ 0 & 0 \\ 0 & 0 \\ 1 & 0 \\ 0 & 1 \end{bmatrix} \begin{bmatrix} \omega_{m-ref} \\ i_{sd-ref} \end{bmatrix} \tag{26}$$

The control law of speed and currents of PMSM is given by the following relationship in (27).

$$\begin{bmatrix} V_{sd^*} \\ V_{sq^*} \end{bmatrix} = -[K_{v\,2\times3} \quad K_{vI\,2\times2}] \begin{bmatrix} i_{sd} \\ i_{sq} \\ \omega_m \\ \zeta_{\omega_m} \\ \zeta_{isd} \end{bmatrix} \tag{27}$$

Fig. 4 shows the block diagram for controlling the speed and currents of the motor using ILQR, where it is noted that it consists of one regulation stage, through which the voltages to be applied to the motor are obtained. The driving system here also includes a SPWM stage to obtain the pulses.

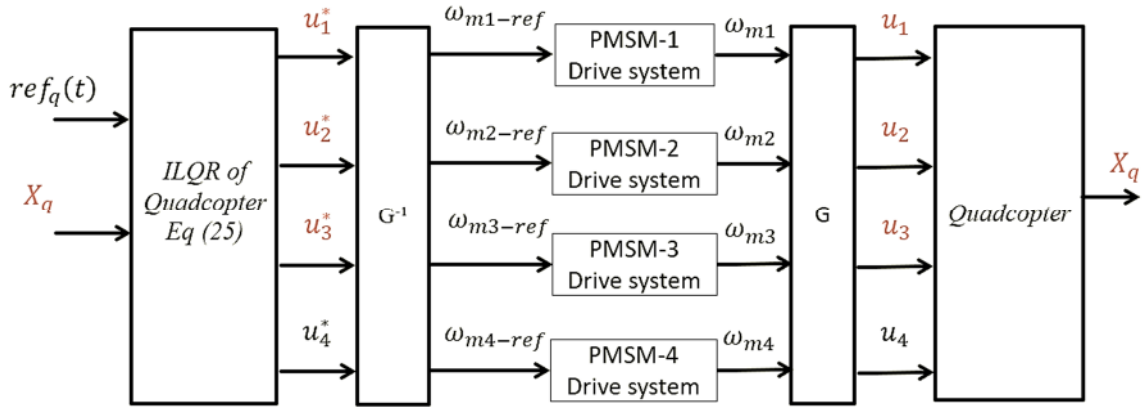

Fig. 2. The block diagram of the complete control system of quadcopter

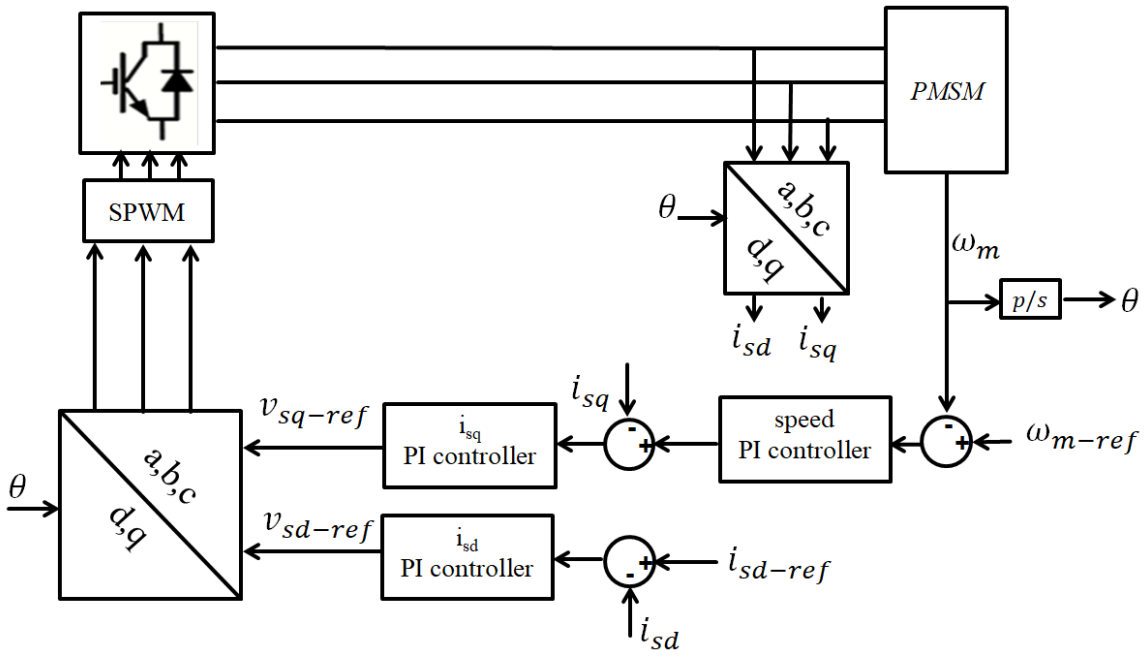

Fig. 3. Sketch of PI control system of PMSM

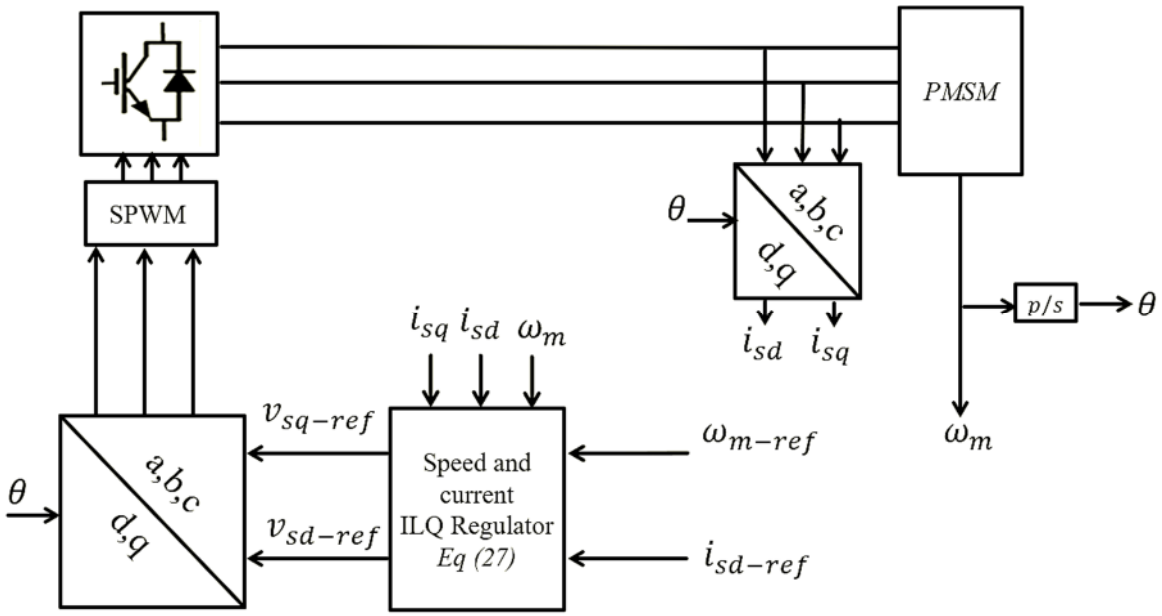

Fig. 4. Sketch of ILQR control system of PMSM

IV. FOC PMSM USING ILQR-PCC

A. Regulating PMSM currents using PCC

Since its initial introduction in the late 1970s, model predictive control, or MPC, has undergone significant development. It has seen a significant advancement in the control research community and industry throughout the past three decades. The reason for MPC's success is that it is, without a doubt, the most universal method for describing the control problem in the time domain [19].

By reducing the error between the reference value and the predicted value, the MPC determines the optimal switching vector [20]. MPC can be applied with different methods, predictive speed controller [21], Model predictive torque control [22], or predictive current control [23].

With the proposed PCC, the inverter produces a consistent number of feasible switching vectors. To do this, the PMSM model is used to estimate, for each switching vector, the currents at the inverter output terminal. Thus, an objective function is designed to select the best switching vector. Reducing the difference between the reference currents and the expected stator currents is the aim of this objective function. There is no longer need for a modulation stage [23].

The difference between the stator's anticipated current ($\overrightarrow{i_p}(k+1)$) and reference currents ($\overrightarrow{i_{ref}}(k+1)$) is calculated by the following objective function in (28).

$$\vec{g} = \overrightarrow{i_{sref}}(k+1) - \overrightarrow{i_{sp}}(k+1)$$

where:

$$\overrightarrow{i_{sref}}(k+1) = \overrightarrow{i_{s\alpha-ref}}(k+1) + J\overrightarrow{i_{s\beta-ref}}(k+1)$$
$$\overrightarrow{i_{sp}}(k+1) = \overrightarrow{i_{s\alpha-p}}(k+1) + J\overrightarrow{i_{s\beta-p}}(k+1) \quad (28)$$

Continuous voltage equation for PMSM can be obtained as follow [20] in (29).

$$\overrightarrow{v_s} = \overrightarrow{i_s}R_s + L_s\frac{d\overrightarrow{i_s}}{dt} + \vec{e} \quad (29)$$

Where $\overrightarrow{v_s}$ refers to the stator voltage generated at the inverter terminal, *Ls* refers to the stator inductance, $\vec{e}$ refers to the back electromotive force. one might estimate the stator current in the subsequent sampling instant for any voltage vector $\overrightarrow{v_s}(x)$ created at the inverter terminal by substituting (di/dt) as in (30).

$$\overrightarrow{i_{sp}}(k+1) = \left(1 - \frac{R_sT_s}{L_s}\right)\overrightarrow{i_s}(k) + \frac{T_s}{L_s}(\overrightarrow{v_s}(k) - \vec{e}(k)) \quad (30)$$

Then, the back electromotive force can be calculated as in (31).

$$\vec{e}(k-1) = \overrightarrow{v_s}(k-1) - (R_s - \frac{L_s}{T_s})\overrightarrow{i_s}(k-1) - \frac{L_s}{T_s}\overrightarrow{i_s}(k) \quad (31)$$

The back electromotive force at present (k) can be estimated, by extrapolating the prior back electromotive force, $\vec{e}(k-1)$. Additionally, because the sample frequency is higher than the back electromotive force frequency, the back electromotive force's magnitude won't fluctuate significantly over the course of a single sampling period. Therefore, $\vec{e}(k) = \vec{e}(k-1)$ is assumed [24].

B. Regulating PMSM speed using ILQR

To design a ILQR for speed control of PMSM, the state space is given as follows in (32):

$$\begin{bmatrix}\dot{\omega_m}\\ \dot{\varepsilon}_{\omega_m}\end{bmatrix} = \begin{bmatrix}\frac{-f}{J} & 0\\ -1 & 0\end{bmatrix}\begin{bmatrix}\omega_m\\ \varepsilon_{\omega_m}\end{bmatrix} + \begin{bmatrix}\frac{1.5p^2\varphi_m}{J}\\ 0\end{bmatrix}[i_{sq}] + \begin{bmatrix}0\\ 1\end{bmatrix}[\omega_{m-ref}] \quad (32)$$

the control law of speed of PMSM is given by the following relationship in (33):

$$[\, i_{sq^*}] = -[K_{i_{1\times1}} \;\; K_{iI_{1\times1}}]\begin{bmatrix}\omega_m\\ \varepsilon_{\omega_m}\end{bmatrix} \quad (33)$$

Fig. 5 shows the block diagram for the ILQR-PCC control system of PMSM, and the Fig. 6 shows the flowchart for implementing the PCC technology.

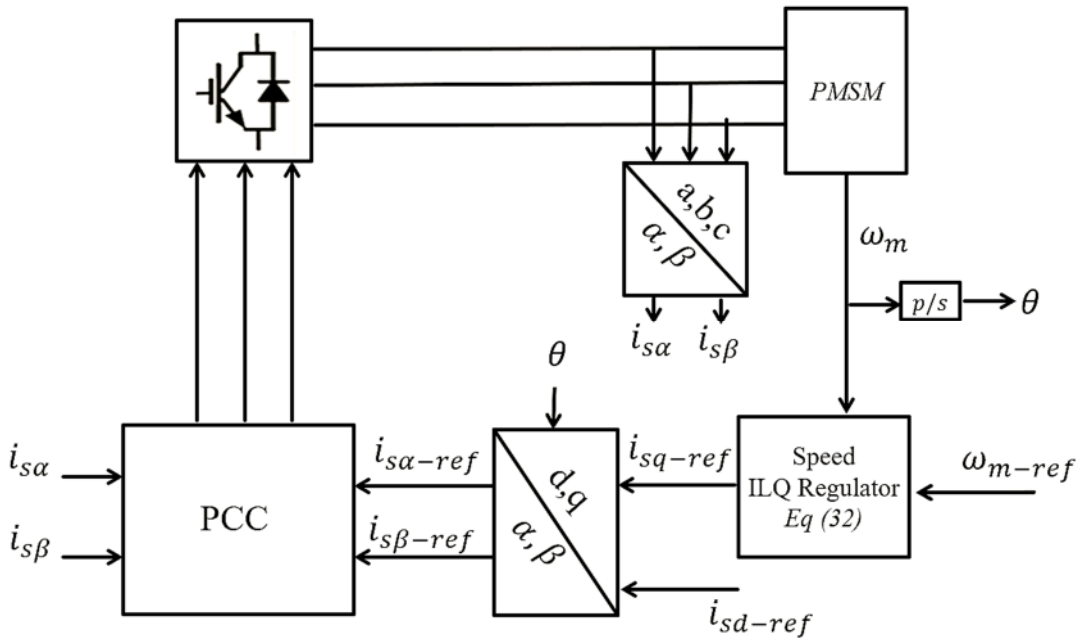

Fig. 5. Sketch of ILQR-PCC control system of PMSM

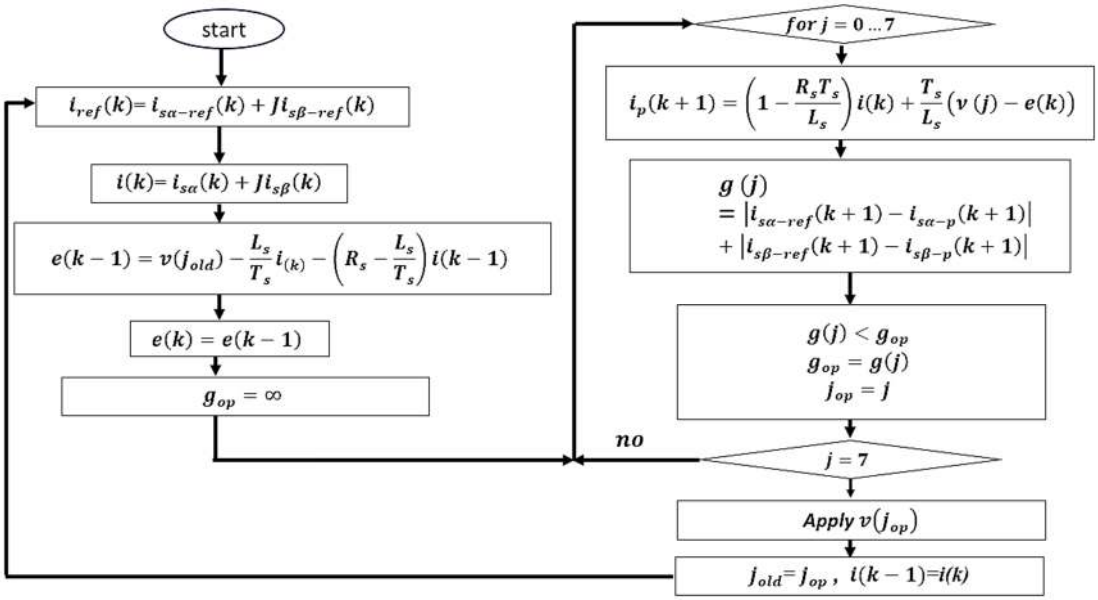

Fig. 6. Flowchart of predictive current control system for PMSM

V. SIMULATIONS RESULTS

To evaluate the performance of the suggested ILQR-PCC system and offer a comparison with alternative control systems, simulation is carried out in Matlab/Simulink environment. Table I displays the PMSM's parameter values.

TABLE I. THE PARAMETER VALUES OF PMSM

stator resistance, Ω	0.33	R_s
inductances stator on d-axis, H	28×10^{-6}	L_d
inductances stator on q-axis, H	28×10^{-6}	L_q
permanent magnet flux, wb	6×10^{-4}	φ_m
number of poles pairs	8	p
inertia torque, Kg.m^2	2.6×10^{-7}	J_r
frictional constant, N.m.rad.sec^{-1}	8.6×10^{-7}	f
Mechanical speed, rad.sec^{-1}	942	ω_m

The reference speed is determined at 450rad/sec from 0sec until 1sec, where its value becomes 900 rad/sec. The load torque is changed from quarter of the nominal torque to the full nominal torque at 0.5sec. Fig. 7 shows the speed regulation response and the Fig. 8 shows the i_{sd} current regulation response.

It is clear from the results shown in Fig. 7 that the proposed control system is superior in terms of response speed and robustness to external disturbance represented by a change in the value of the load torque. It is also clear from Fig. 8, that the proposed control system is superior in reducing current fluctuations, which was regulated at 0A.

To further verify the effectiveness of the proposed system in reducing current and torque ripples, the two Fig. 9 and Fig. 10 show a comparison between PMSM currents and electromagnetic torque respectively for using the three control systems.

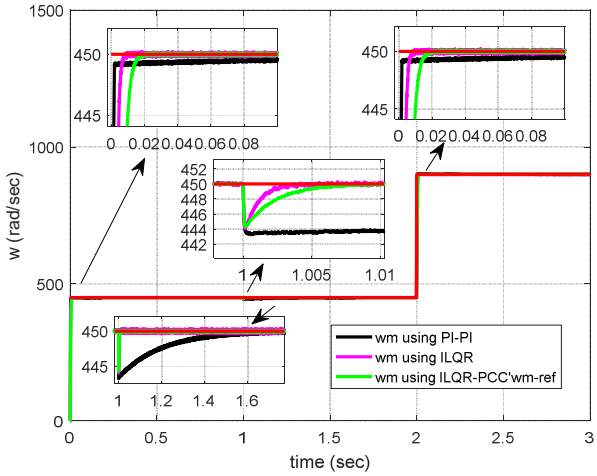

Fig. 7. The speed regulation response

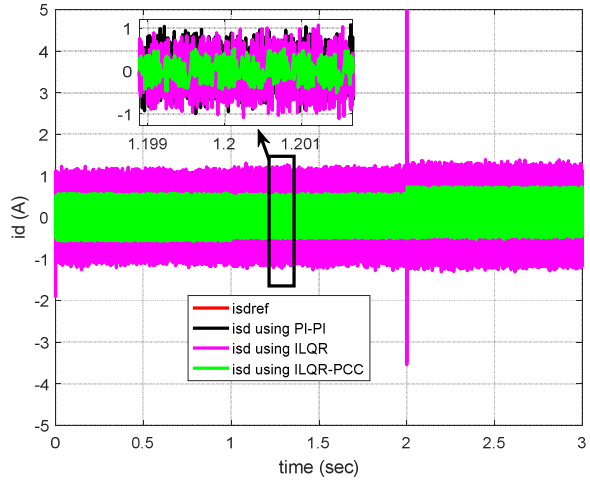

Fig. 8. The i_{sd} current regulation response

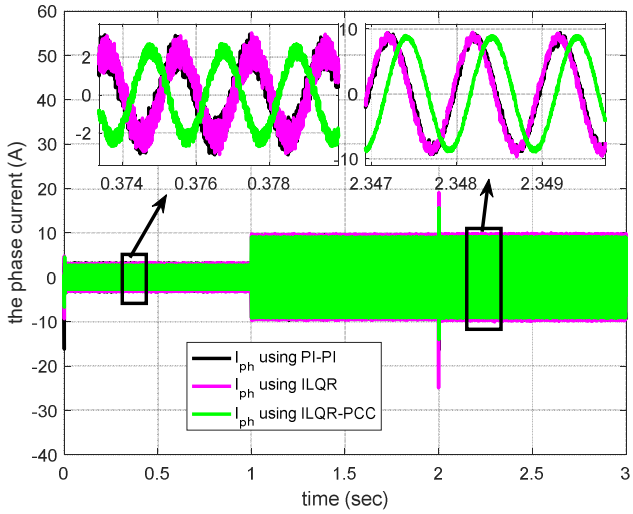

Fig. 9. Comparison of the current waveform when using the three control systems

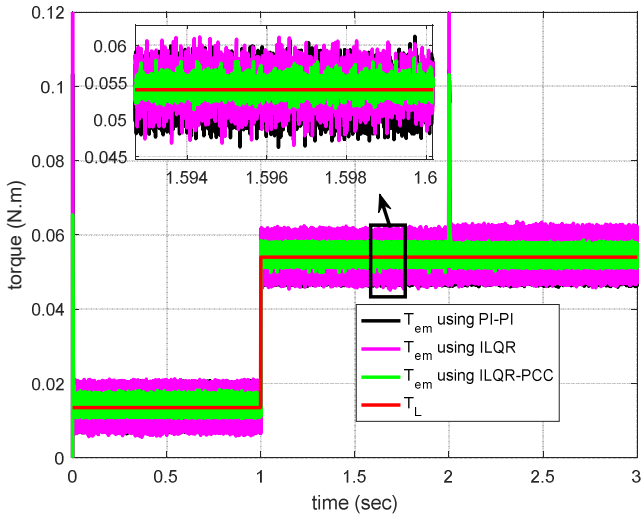

Fig. 10. A comparison between the response of the electromagnetic torque when using the three control systems

It is clear from the results presented in Fig. 9 and Fig. 10 that the effectiveness of using the proposed control system is evident, it contributes to reducing current distortions, and the electromagnetic torque ripples have the lowest value compared to other control systems.

A simulation was performed regarding the operation of the PMSM drive system within a quadcopter, with full load torque applied to the PMSM. Fig. 11 to Fig. 14 show the response of the quadcopter control system to follow the desired path. Fig. 15 shows the speeds of the four motors. Fig. 16 to Fig. 18 show the response of the first motor drive system to regulate speed, current, and torque.

It is clear by reviewing the results in Fig. 11 to Fig. 14 that the quadcopter control system is effective, as the desired path is tracked with high accuracy and dynamism. As is clear from Fig. 15, the speeds of the four motors are different within small limits to ensure the correct guidance of the quadcopter to the desired position. The effectiveness of the aircraft control system and tracking the desired path inevitably means the effectiveness of the engine speed control system, as shown by the results in Fig. 16 to Fig. 18. It is noted that the reference signals are tracked accurately and quickly, with low ripples for both the motor current and torque.

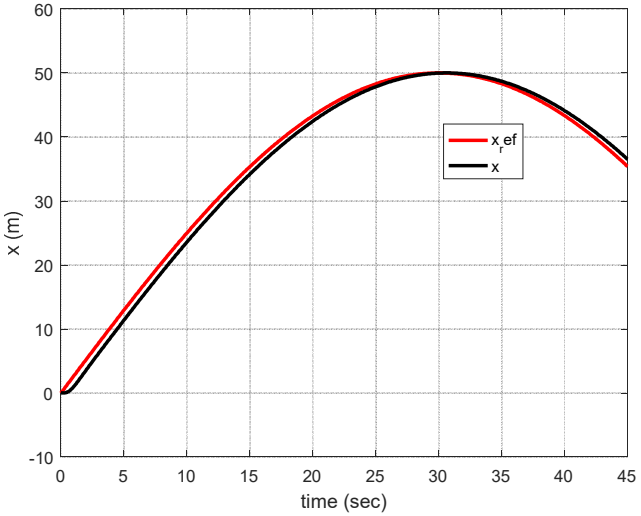

Fig. 11. . response of quadcopter on the x-axis

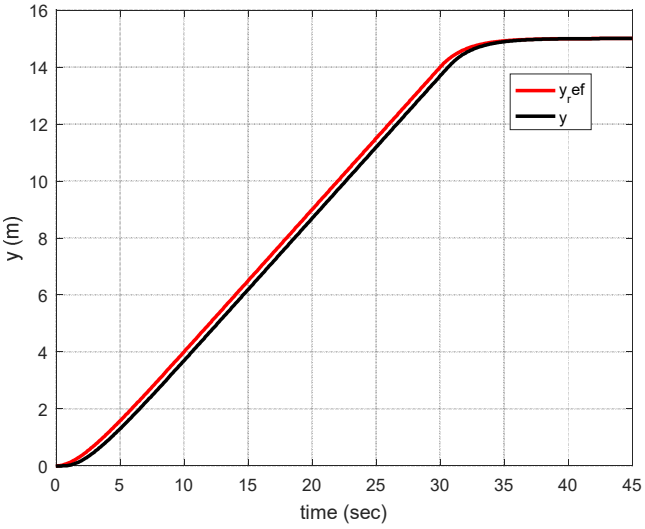

Fig. 12. Response of quadcopter on the y-axis

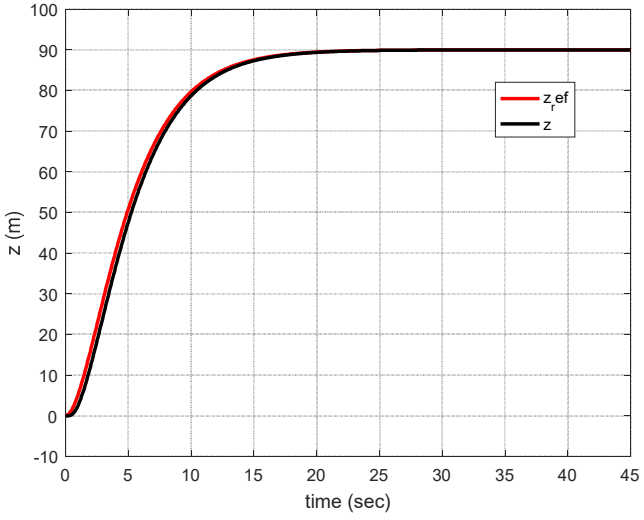

Fig. 13. Response of quadcopter on the z-axis

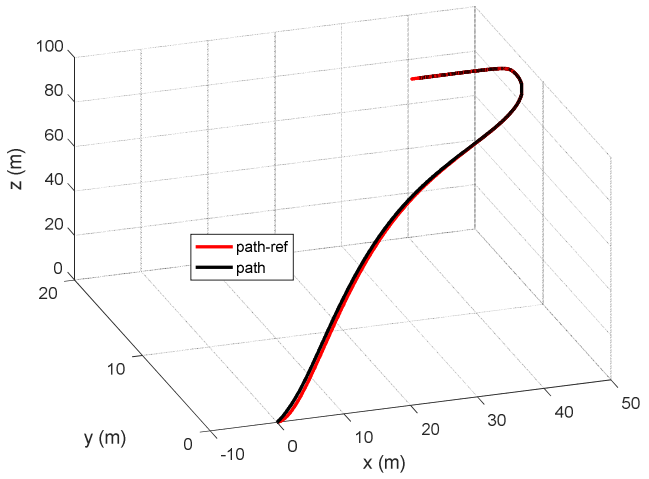

Fig. 14. Response on xyz space

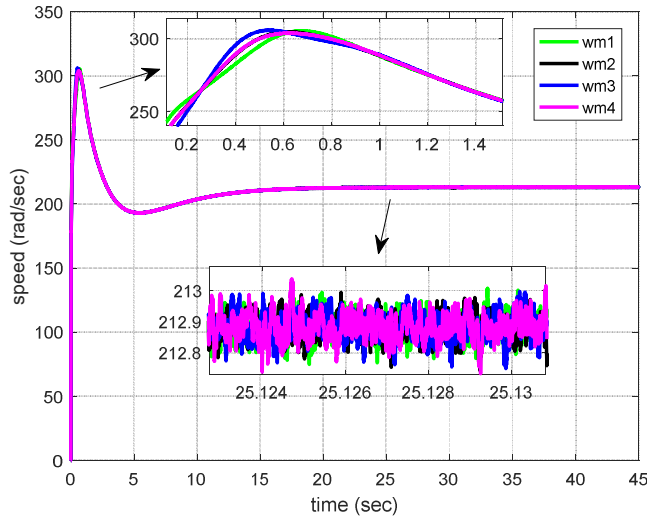

Fig. 15. The speeds of the four motors

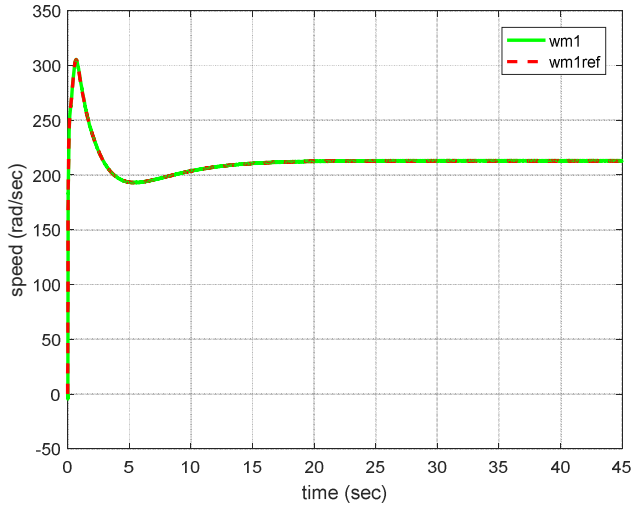

Fig. 16. The speed response of the first motor drive system operating in quadcopter

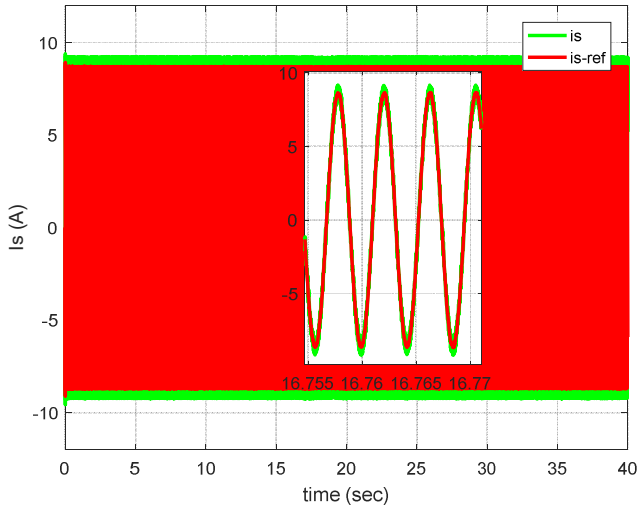

Fig. 17. The current response of the first motor drive system operating in quadcopter

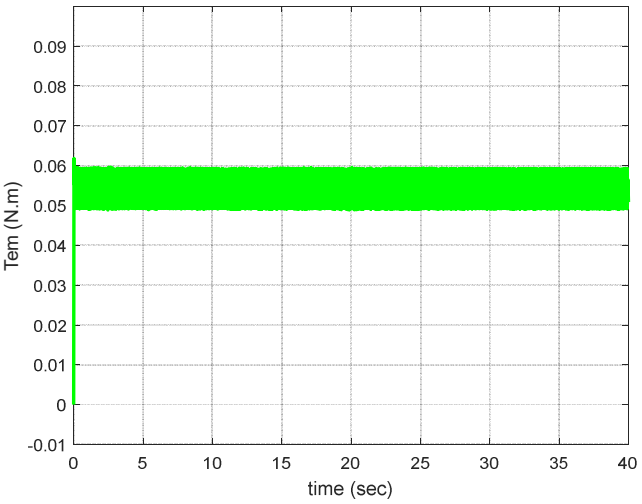

Fig. 18. The torque response of the first motor drive system operating in quadcopter

VI. CONCLUSION

In this paper, the author develops a new strategy for controlling the Permanent Magnet Synchronous Motor (PMSM) control system with an objective of having a stable dynamic response and least torque fluctuations. The proposed control system is composed of an ILQR for speed regulation and PCC and is a significant improvement over conventional control strategy. The effectiveness of the ILQR-PCC control system was rigorously evaluated by comparing its performance against two established control systems: The comparison is made between the ILQR and the Proportional-Integral (PI) control system.

The detailed comparison of the comparative metrics is presented in Table II, where one can note the advantage of the ILQR-PCC control system. In other words, the performance of the ILQR-PCC system was characterized by; a measurable improvement in the system's dynamic response, better disturbance attenuation capabilities, and reduced current waveform distortions which compiled to the reduction of torque ripples. Nevertheless, the PI and ILQR control systems cannot compete with the ILQR-PCC system,

especially in the cases when high dynamic stability and accurate definition of current regulation is needed.

This was again proven when the ILQR-PCC control system was implemented in an LQR-controlled quadcopter. This experimental analysis substantiated that the system's capability to follow reference signals was fast and precise while concurrently keeping minor current distortion. Another area where improved control capability was apparent was in the aircraft's capacity to track the desired attitude flight profile with lot of precision and quickness.

TABLE II. COMPARISON BETWEEN THE THREE SYSTEMS

Control system	System performance in speed regulation		Current and torque ripples
	settling time	required time to overcome external disturbance	
PI-PI	0.35sec	0.6sec	high
ILQR	0.02sec	0.01sec	high
ILQR-PCC	0.01sec	0.006sec	low

Owing to these findings, there is potential in enhancing the ILQR-PCC control system for improved operation of the PMSM driven applications, especially in areas that need specific speed and accurate control as in flight of the quadcopter. It may be beneficial for future works to extend the described control strategy to other similar systems, assess the methodology's performance when coping with higher dimensional or multiscale systems, in addition to discussing how possible shortcomings such as computation time and real-time requirements may be overcome.

REFERENCES

[1] O. Araar and N. Aouf, "Quadrotor control for trajectory tracking in presence of wind disturbances," *2014 UKACC International Conference on Control (CONTROL)*, pp. 25-30, 2014, doi: 10.1109/CONTROL.2014.6915110.

[2] D. Bazylev, A. Margun, K. Zimenko and A. Kremlev, "UAV equipped with a robotic manipulator," *22nd Mediterranean Conference on Control and Automation*, Palermo, Italy, 2014, pp. 1177-1182, doi: 10.1109/MED.2014.6961535.

[3] I. Palunko and R. Fierro, "Adaptive control of a quadrotor with dynamic changes in the center of gravity," *IFAC Proceedings Volumes*, vol. 44, no. 1, pp. 2626-2631, 2011.

[4] K. Issam and G. Qingbo, "Research on control strategies for the stabilization of quadrotor UAV," *Fifth International Conference on Intelligent Control and Information Processing*, pp. 286-292, 2014, doi: 10.1109/ICICIP.2014.7010265.

[5] R. Kumar, A. M. Deshpande, J. Z. Wells, and M. Kumar, "Flight Control of Sliding Arm Quadcopter with Dynamic Structural Parameters," *2020 IEEE/RSJ International Conference on Intelligent Robots and Systems (IROS)*, pp. 1358-1363, 2020, doi: 10.1109/IROS45743.2020.9340694.

[6] O. Harkare and R. Maan, "Design and Control of a Quadcopter," *Int. J. Eng. Tech. Res*, vol. 10, no. 5, 2021.

[7] A. Tagay, A. Omar, and M. H. Ali, "Development of control algorithm for a quadcopter," *Procedia Computer Science*, vol. 179, pp. 242-251, 2021.

[8] M. H. Kebedew and S. Kim, "Improved Speed Control through Model Predictive Techniques for Permanent Magnet Synchronous Motor in Electric Vehicles," *Daagu International Journal of Basic and Applied research (DIJBAR)*, vol. 6, no. 1, pp. 435-450, 2024.

[9] I. Chinaeke-Ogbuka *et al*., "A robust high-speed sliding mode control of permanent magnet synchronous motor based on simplified hysteresis current comparison," *International Journal of Power Electronics and Drive Systems*, vol. 12, no. 1, 2021.

[10] M. Hassan, X. Ge, R. Atif, A. T. Woldegiorgis, M. S. Mastoi, and M. B. Shahid, "Computational efficient model predictive current control for interior permanent magnet synchronous motor drives," *IET Power Electronics*, vol. 15, no. 12, pp. 1111-1133, 2022.

[11] C. O. Omeje, A. O. Salau, and C. U. Eya, "Dynamics analysis of permanent magnet synchronous motor speed control with enhanced state feedback controller using a linear quadratic regulator," *Heliyon*, vol. 10, no. 4, 2024.

[12] M. Nicola and C. -I. Nicola, "Improved Performance for PMSM Control System Based on LQR Controller and Computational Intelligence," *2021 International Conference on Electrical, Computer and Energy Technologies (ICECET)*, pp. 1-6, 2021, doi: 10.1109/ICECET52533.2021.9698758.

[13] N. P. Nguyen, N. X. Mung, H. L. N. N. Thanh, T. T. Huynh, N. T. Lam, and S. K. Hong, "Adaptive Sliding Mode Control for Attitude and Altitude System of a Quadcopter UAV via Neural Network," in *IEEE Access*, vol. 9, pp. 40076-40085, 2021, doi: 10.1109/ACCESS.2021.3064883.

[14] F. Ahmad, P. Kumar, A. Bhandari, and P. P. Patil, "Simulation of the Quadcopter Dynamics with LQR based Control," *Materials Today: Proceedings*, vol. 24, pp. 326-332, 2020.

[15] O. Araar and N. Aouf, "Full linear control of a quadrotor UAV, LQ vs H∞," *2014 UKACC International Conference on Control (CONTROL)*, pp. 133-138, 2014, doi: 10.1109/CONTROL.2014.6915128.

[16] H. M. Soliman and S. M. L. Hakim, "Simple Model and PI Controller to Improve the Performance Characteristics of PMSM under Field Oriented Control with Using SVPWM," *Int. J. Adv. Eng. Nano Technol*, vol. 2, pp. 5-13, 2015.

[17] R. Na and X. Wang, "An Improved Vector-Control System of PMSM Based on Fuzzy Logic Controller," *2014 International Symposium on Computer, Consumer and Control*, pp. 326-331, 2014, doi: 10.1109/IS3C.2014.92.

[18] K. Li, X. Liu, J. Sun, and C. Zhang, "Robust current control of PMSM based on PCH and disturbance observer," *Proceedings of the 33rd Chinese Control Conference*, pp. 7938-7942, 2014, doi: 10.1109/ChiCC.2014.6896326.

[19] F. Shiravani, P. Alkorta, J. A. Cortajarena, and O. Barambones, "An improved predictive current control for IM drives," *Ain Shams Engineering Journal*, vol. 14, no. 8, p.102037, 2023.

[20] P. Kakosimos and H. Abu-Rub, "Predictive Speed Control With Short Prediction Horizon for Permanent Magnet Synchronous Motor Drives," in *IEEE Transactions on Power Electronics*, vol. 33, no. 3, pp. 2740-2750, March 2018, doi: 10.1109/TPEL.2017.2697971.

[21] X. Sun *et al*., "MPTC for PMSMs of EVs With Multi-Motor Driven System Considering Optimal Energy Allocation," in *IEEE Transactions on Magnetics*, vol. 55, no. 7, pp. 1-6, July 2019, doi: 10.1109/TMAG.2019.2904289.

[22] A. Devanshu, M. Singh, and N. Kumar, "Adaptive predictive current control of field-oriented controlled induction motor drive," *IETE Journal of Research*, vol. 68, no. 5, pp. 3707-3719, 2022.

[23] A. Devanshu, M. Singh, and N. Kumar, "An Improved Nonlinear Flux Observer Based Sensorless FOC IM Drive With Adaptive Predictive Current Control," in *IEEE Transactions on Power Electronics*, vol. 35, no. 1, pp. 652-666, Jan. 2020, doi: 10.1109/TPEL.2019.2912265.

[24] S. A. Ahmed *et al*., "Advancements in UAV image semantic segmentation: A comprehensive literature review," *Multidisciplinary Reviews*, vol. 7, no. 6, pp. 2024118-2024118, 2024.

[25] I. Şahin and C. Ulu, "Altitude control of a quadcopter using interval type-2 fuzzy controller with dynamic footprint of uncertainty," *ISA transactions*, vol. 134, pp. 86-94, 2023.

[26] A. J. Abougarair, H. Almgallesh, and N. A. A. Shashoa, "Dynamics and Optimal Control of Quadcopter," *2024 IEEE 4th International Maghreb Meeting of the Conference on Sciences and Techniques of Automatic Control and Computer Engineering (MI-STA)*, pp. 136-141, 2024, doi: 10.1109/MI-STA61267.2024.10599742.

[27] R. Elagib and A. Karaarslan, "Sliding mode control-based modeling and simulation of a quadcopter," *J. Eng. Res. Rep*, vol. 24, no. 3, pp. 32-41, 2023.

[28] T. A. Taha, H. I. Zaynal, A. S. T. Hussain, H. Desa, and F. H. Taha, "Definite time over-current protection on transmission line using

MATLAB/Simulink," *Bulletin of Electrical Engineering and Informatics*, vol. 13, no. 2, pp. 713-723, 2024.

[29] A. Azka, A. Santoso, and T. Agustinah, "Controlling a Quadcopter with Static Loads and Dynamic Wind Disturbances using a Fuzzy Inference System," *JAREE (Journal on Advanced Research in Electrical Engineering)*, vol. 8, no. 2, 2024.

[30] W. J. Elke and R. Caverly, "Dynamics, Guidance, and Control of a Low-Cost Quadcopter-Based Space Vehicle Testbed," in *AIAA SCITECH 2024 Forum*, p. 0778, 2024.

[31] L. Cedro, K. Wieczorkowski, and A. Szcześniak, "An Adaptive PID Control System for the Attitude and Altitude Control of a Quadcopter," *acta mechanica et automatica*, vol. 18, no. 1, pp. 29-39, 2024.

[32] M. Merzban, A. A. Khalaf, and H. F. A. Hamed, "Comparison of various control techniques applied to a quadcopter," *Journal of Advanced Engineering Trends*, vol. 42, no. 2, pp. 233-244, 2023.

[33] Y. Li, B. Peng, L. He, K. Fan, Z. Li, and L. Tong, "Road extraction from unmanned aerial vehicle remote sensing images based on improved neural networks," *Sensors*, vol. 19, no. 19, p. 4115, 2019.

[34] J. W. Lee, N. Xuan-Mung, N. P. Nguyen, and S. K. Hong, "Adaptive altitude flight control of quadcopter under ground effect and time-varying load: Theory and experiments," *Journal of Vibration and Control*, vol. 29, no. 3-4, pp. 571-581, 2023.

[35] A. Belmouhoub, Y. Bouzid, S. Medjmadj, S. H. Derrouaoui, H. Siguerdidjane, and M. Guiatni, "Fast terminal synergetic control for morphing quadcopter with time-varying parameters," *Aerospace Science and Technology*, vol. 141, p. 108540, 2023.

[36] S. Srey and S. Srang, "Adaptive Controller Based on Estimated Parameters for Quadcopter Trajectory Tracking," *International Journal of Robotics & Control Systems*, vol. 4, no. 2, 2024.

[37] B. S. Guevara, L. F. Recalde, J. Varela-Aldás, D. C. Gandolfo, and J. M. Toibero, "Quadcopters Control Using Online Dynamic Mode Decomposition," *IFAC-PapersOnLine*, vol. 56, no. 3, pp. 589-594, 2023.

[38] S. R. Ahmed, M. F. Khaleel, B. A. Abubaker, S. K. Sulaiman, A. S. T. Hussain, T. A. Taha, and M. Fadhil, "Deep Convolutional Neural Network (DCNN) for the Identification of Striping in Images of Blood Cells," in *International Conference on Forthcoming Networks and Sustainability in the AIoT Era*, pp. 83-89, 2024.

[39] Y. Li, Q. Zhu, and A. Elahi, "Quadcopter Trajectory Tracking Control Based on Flatness Model Predictive Control and Neural Network," in *Actuators*, vol. 13, no. 4, p. 154, 2024.

[40] L. Chen, J. Zhang, and Q. Quan, "Quadcopter attitude control with vibration reduction by additive-state-decomposition dynamic inversion design with a notch filter," *Nonlinear Dynamics*, vol. 111, no. 9, pp. 8313-8327, 2023.

[41] A. Fekik *et al*., "Modeling and Simulation of Quadcopter Using Self-tuning Fuzzy-PI Controller," in *Mobile Robot: Motion Control and Path Planning*, pp. 231-251, 2023.

[42] V. Alexandrov, I. Rezkov, D. Shatov, and Y. Morozov, "Frequency Domain Identification of the Quadcopter Attitude Dynamics," *Advances in Systems Science and Applications*, vol. 23, no. 3, pp. 1-15, 2023.

[43] O. F. Awad, S. R. Ahmed, A. S. Shaker, D. A. Majeed, A. S. T. Hussain, and T. A. Taha, "Human Activity Recognition Using Convolutional Neural Networks," in *International Conference on Forthcoming Networks and Sustainability in the AIoT Era*, pp. 258-274, 2024.

[44] N. J. Kong, C. Li, G. Council, and A. M. Johnson, "Hybrid iLQR Model Predictive Control for Contact Implicit Stabilization on Legged Robots," in *IEEE Transactions on Robotics*, vol. 39, no. 6, pp. 4712-4727, Dec. 2023, doi: 10.1109/TRO.2023.3308773.

[45] Z. Huang, S. Shen, and J. Ma, "Decentralized iLQR for Cooperative Trajectory Planning of Connected Autonomous Vehicles via Dual Consensus ADMM," in *IEEE Transactions on Intelligent Transportation Systems*, vol. 24, no. 11, pp. 12754-12766, Nov. 2023, doi: 10.1109/TITS.2023.3286898.

[46] X. Kong, W. Ning, Y. Xia, Z. Sun, and H. Xie, "Adaptive High-Order Control Barrier Function-Based Iterative LQR for Real Time Safety-Critical Motion Planning," in *IEEE Robotics and Automation Letters*, vol. 9, no. 7, pp. 6099-6106, July 2024, doi: 10.1109/LRA.2024.3398506.

[47] B. H. Chen and P. C. Lin, "Deep Imitation Learning for Optimal Trajectory Planning and Initial Condition Optimization for an Unstable Dynamic System," *Advanced Intelligent Systems*, vol. 6, no. 1, p. 2300379, 2024.

[48] T. A. Taha, A. S. T. Hussain, H. Desa, F. H. Taha, and Y. Bektaş, "Child tracking system using smartphone," *Bulletin of Electrical Engineering and Informatics*, vol. 12, no. 5, pp. 2745-2752, 2023.

[49] Z. Williams, J. Chen and N. Mehr, "Distributed Potential iLQR: Scalable Game-Theoretic Trajectory Planning for Multi-Agent Interactions," *2023 IEEE International Conference on Robotics and Automation (ICRA)*, pp. 1-7, 2023, doi: 10.1109/ICRA48891.2023.10161176.

[50] S. Sugiura, R. Ariizumi, M. Tanemura, T. Asai, and S. I. Azuma, "Data-driven estimation of the algebraic Riccati equation for the discrete-time inverse linear quadratic regulator problem," *Discover Applied Sciences*, vol. 6, no. 6, p. 284, 2024.

[51] A. Sharma and S. Chakravorty, "A Reduced Order Iterative Linear Quadratic Regulator (ILQR) Technique for the Optimal Control of Nonlinear Partial Differential Equations," *2023 American Control Conference (ACC)*, pp. 3389-3394, 2023, doi: 10.23919/ACC55779.2023.10156062.

[52] L. Pedroso and P. Batista, "Discrete-time decentralized linear quadratic control for linear time-varying systems," *International Journal of Robust and Nonlinear Control*, vol. 33, no. 1, pp. 67-101, 2023.

[53] T. A. Taha, M. K. Hassan, H. I. Zaynal, and N. I. A. Wahab, "Big Data for Smart Grid: A Case Study," in *Big Data Analytics Framework for Smart Grids*, pp. 142-180, 2024.

[54] D. Zhao, X. Yang, Y. Li, L. Xu, J. She, and S. Yan, "A Kalman–Koopman LQR Control Approach to Robotic Systems," in *IEEE Transactions on Industrial Electronics*, pp. 1-10, 2024, doi: 10.1109/TIE.2024.3379674.

[55] Y. Liu, X. Pei, H. Zhou, and X. Guo, "Spatiotemporal Trajectory Planning for Autonomous Vehicle Based on Reachable Set and Iterative LQR," in *IEEE Transactions on Vehicular Technology*, vol. 73, no. 8, pp. 10932-10947, Aug. 2024, doi: 10.1109/TVT.2024.3371184.

[56] Q. Zhang, A. Taghvaei, and Y. Chen, "An optimal control approach to particle filtering," *Automatica*, vol. 151, p. 110894, 2023.

[57] A. -S. T. Hussain, M. Fadhil, T. A. Taha, O. K. Ahmed, S. A. Ahmed, and H. Desa, "GPS and GSM Based Vehicle Tracking System," *2023 7th International Symposium on Innovative Approaches in Smart Technologies (ISAS)*, pp. 1-5, 2023, doi: 10.1109/ISAS60782.2023.10391720.

[58] Z. Chen, B. Wang, C. Wang, Y. Wang, P. Xiao, and K. Li, "Performance of a Subgrade-Embankment-Seawall System Reinforced by Drainage PCC Piles and Ordinary Piles Subjected to Lateral Spreading," *Geofluids*, vol. 2023, no. 1, p. 4489478, 2023.

[59] M. Hosseinpour, M. J. Shojaei, M. Salimi, and M. Amidpour, "Machine learning in absorption-based post-combustion carbon capture systems: A state-of-the-art review," *Fuel*, vol. 353, p. 129265, 2023.

[60] S. Ali, J. Wang, and V. C. M. Leung, "Defensive strategies against PCC attacks based on ideal (t, n)-secret sharing scheme," *Journal of King Saud University-Computer and Information Sciences*, vol. 35, no. 9, p. 101784, 2023.

[61] A. -S. T. Hussain, T. A. Taha, S. R. Ahmed, S. A. Ahmed, O. K. Ahmed, and H. Desa, "Automated RFID-Based Attendance and Access Control System for Efficient Workforce Management," *2023 7th International Symposium on Innovative Approaches in Smart Technologies (ISAS)*, pp. 1-6, 2023, doi: 10.1109/ISAS60782.2023.10391615.

[62] Q. Yu, X. Cao, X. Deng, T. Zhu, Z. Deng, and C. Liu, "An Improved Control Strategy to Reduce Torque Spikes and Ripple for Bearingless Switched Reluctance Motors," in *IEEE Transactions on Industrial Informatics*, vol. 20, no. 4, pp. 5147-5159, April 2024, doi: 10.1109/TII.2023.3326529.

[63] M. S. Rafaq, W. Midgley, and T. Steffen, "A Review of the State of the Art of Torque Ripple Minimization Techniques for Permanent Magnet Synchronous Motors," in *IEEE Transactions on Industrial Informatics*, vol. 20, no. 1, pp. 1019-1031, Jan. 2024, doi: 10.1109/TII.2023.3272689.

[64] A. M. Abou-ElSoud, A. S. A. Nada, A. A. M. Abdel-Aziz, and W. Sabry, "Torque ripples reduction of electric vehicle synchronous reluctance motor drive using the strong action controller," *Ain Shams Engineering Journal*, vol. 15, no. 2, p. 102428, 2024.

[65] D. -H. Choi, D. -H. Kim, H. -S. Han, D. -H. Jung, and W. -H. Kim, "Design of a Slotless Structure for Minimizing Cogging Torque and Torque Ripple in a Column Type EPS Motor for Vehicles," in *IEEE Transactions on Magnetics*, vol. 60, no. 9, pp. 1-5, Sept. 2024, doi: 10.1109/TMAG.2024.3428343.

[66] M. A. Hoque, M. K. Hassan, A. Hajjo, and T. A. Taha, "Investigation of Battery Energy Storage System (BESS) during Loading Variation," *Journal of Advanced Research in Applied Mechanics*, vol. 110, no. 1, pp. 86-96, 2023.

[67] A. Abdel-Aziz, M. Elgenedy, and B. Williams, "Review of switched reluctance motor converters and torque ripple minimisation techniques for electric vehicle applications," *Energies*, vol. 17, no. 13, p. 3263, 2024.

[68] H. Masoudi, A. Kiyoumarsi, S. M. Madani, and M. Ataei, "Torque Ripple Reduction of Nonsinusoidal Brushless DC Motor Based on Super-Twisting Sliding Mode Direct Power Control," in *IEEE Transactions on Transportation Electrification*, vol. 9, no. 3, pp. 3769-3779, Sept. 2023, doi: 10.1109/TTE.2023.3250950.

[69] Q. Chen, Z. Xu, Y. Hu, J. Ding, and Y. Xie, "Research on torque ripple optimization of permanent magnet synchronous motor for electric vehicle based on modular poles," *IEEJ Transactions on Electrical and Electronic Engineering*, vol. 18, no. 4, pp. 613-622, 2023.

[70] N. Prabhu, R. Thirumalaivasan, and B. Ashok, "Critical Review on Torque Ripple Sources and Mitigation Control Strategies of BLDC Motors in Electric Vehicle Applications," in *IEEE Access*, vol. 11, pp. 115699-115739, 2023, doi: 10.1109/ACCESS.2023.3324419.

[71] E. Bektaş *et al*., "Enhancing Harmonic Reduction in Multilevel Inverters using the Weevil Damage Optimization Algorithm," *Journal of Robotics and Control (JRC)*, vol. 5, no. 3, pp. 717-722, 2024.

[72] D. H. Choi, I. J. Yang, M. K. Hong, D. H. Jung, and W. H. Kim, "High-Speed Design with Separated Tapering for Reducing Cogging Torque and Torque Ripple of a 3 kW Dry Vacuum Pump Motor for the ETCH Process," *Machines*, vol. 11, no. 11, p. 991, 2023.

[73] X. Li, Z. Sun, W. Sun, L. Guo, and H. Wang, "Design of permanent magnet-assisted synchronous reluctance motor with low torque ripple," *World Electric Vehicle Journal*, vol. 14, no. 4, p. 82, 2023.

[74] L. Zhang, Z. Cui, P. Song, L. Wang, and X. Liu, "Sinusoidal Rotor Core Shape for Low Torque Ripple in Hollow-Cup Machines," *Energies*, vol. 17, no. 13, p. 3168, 2024.

[75] S. Masoudi, L. Ben-Brahim, A. Gastli, N. Al-Emadi, and M. Djemai, "Reducing Force Ripples and Enhancing Reliability in LSRMs Through Modern Structure and Advanced Control Systems," in *IEEE Access*, vol. 12, pp. 50114-50125, 2024, doi: 10.1109/ACCESS.2024.3385437.

[76] A. S. T. Hussain *et al*., "Unlocking Solar Potential: Advancements in Automated Solar Tracking Systems for Enhanced Energy Utilization," *Journal of Robotics and Control (JRC)*, vol. 5, no. 4, pp. 1018-1027, 2024.

[77] Q. Yu, X. Cao, Z. Deng, X. Deng and C. Liu, "An Improved Direct Displacement Control for Bearingless Switched Reluctance Motors to Reduce Torque Ripple and Improve Levitation Performance," in *IEEE Transactions on Energy Conversion*, pp. 1-12, 2024, doi: 10.1109/TEC.2024.3393502.

[78] T. Ben, H. Wang, L. Chen, Y. Zhang, and L. Jing, "Torque ripple reduction strategy for switched reluctance motor based on segmented non-linear correction torque sharing function," *Journal of Power Electronics*, pp. 1-11, 2024.

[79] J. Croonen, A. L. J. Deraes, J. Beckers, W. Devesse, O. Hegazy, and B. Verrelst, "Active Torque Control for Speed Ripple Elimination: A Mechanical Perspective," *Machines*, vol. 12, no. 4, p. 222, 2024.

[80] H. Juma'a and T. Atyia, "Design and Implementation of multi-level inverter for PV system with various DC Sources," *NTU Journal of Renewable Energy*, vol. 5, no. 1, pp. 24-33, 2023.

[81] N. H. Aziz, "Load Frequency Control With Renewable Energy Sources Using Practical Swarm Optimization Based On PID," *NTU Journal of Renewable Energy*, vol. 5, no. 1, pp. 61-73, 2023.

[82] F. M. Mahmood, S. S. Jaafar, R. W. Mustafa, Y. H. Azeez, and B. K. Mahmood, "Design and Programming of a Microcontroller Based on a Solar Tracking System," *NTU Journal of Renewable Energy*, vol. 3, no. 1, pp. 51-59, 2022.

[83] T. A. Taha *et al*., "Enhancing Multilevel Inverter Performance: A Novel Dung Beetle Optimizer-based Selective Harmonic Elimination Approach," *Journal of Robotics and Control (JRC)*, vol. 5, no. 4, pp. 944-953, 2024.

[84] T. T. Nguyen, T. H. Nguyen, and J. W. Jeon, "Explicit Model Predictive Speed Control for Permanent Magnet Synchronous Motor With Torque Ripple Minimization," in *IEEE Access*, vol. 11, pp. 134199-134210, 2023, doi: 10.1109/ACCESS.2023.3335992.

[85] T. Banerjee and J. N. Bera, "An improved torque ripple reduction controller for smooth operation of induction motor drive," *Journal of Control, Automation and Electrical Systems*, vol. 34, no. 2, pp. 247-264, 2023.

[86] S. T. Bahar and R. G. Omar, "Permanent Magnet Synchronous Motor Torque Ripple Reduction Using Predictive Torque Control," *Journal of Engineering and Sustainable Development*, vol. 27, no. 3, pp. 394-406, 2023.

[87] T. A. Taha, N. I. A. Wahab, M. K. Hassan, and H. I. Zaynal, "Selective Harmonic Elimination in Multilevel Inverters Using the Bonobo Optimization Algorithm," in *International Conference on Forthcoming Networks and Sustainability in the AIoT Era*, pp. 304-321, 2024.